



Field-effect transition sensor for KI detection based on self-assembled calixtube monolayers



Kirill Puchnin^{a,b,*}, Mariia Andrianova^b, Alexander Kuznetsov^b, Vladimir Kovalev^a

^a Department of Chemistry, M.V. Lomonosov Moscow State University, 1–3 Leninskiye Gory, GSP-1, Moscow 119991, Russia

^b Scientific-Manufacturing Complex Technological Center, 1–7 Shokin Square, Zelenograd, Moscow 124498, Russia

ARTICLE INFO

Keywords:

Calixarene

Thin film

Host-guest system

ISFET

Potassium iodide

Self-assembled monolayer

ABSTRACT

A series of novel calixarene-based tubes comprising different numbers of silatrane anchoring groups was synthesized. For the first time, a self-assembled monolayer (SAM) derived from calixtubes was formed on a SiO₂ surface. The formation of the SAM was confirmed by X-ray photoelectron spectroscopy, scanning electron microscopy-energy dispersive X-ray analysis, and contact angle measurements. Modification of the sensitive surface of a conventional ion-selective field effect transistor (ISFET) with the afforded SAM resulted in the production of a KI-sensitive sensor. This sensor selectively determined KI compare to different alkali metal iodides: NaI, RbI, CsI; also investigation of different potassium salts (acetate, iodide, nitrate, chloride, dihydrophosphate, perchlorate) showed the highest response to KI. This sensor was successfully employed to determine the presence of KI in artificial saliva with a limit of detection of $\sim 3 \times 10^{-8}$ M. In addition, it was found that the detection limit of the sensor could be increased by combining the sensor with a microfluidic system. Due to the obtained sensor sensitivity and its ability to detect KI in artificial saliva, we could conclude that this sensor shows great potential for application in the determination of KI in different media, such as the human body and in biological liquids, such as saliva or urine.

1. Introduction

The detection and identification of different compounds is a key issue in modern applied chemistry, with potassium iodide being of particular interest due to its role as a drug for treating dermatologic diseases. More specifically, potassium iodide is successfully employed in the treatment of inflammatory dermatoses, most notably erythema nodosum, subacute nodular migratory panniculitis, nodular vasculitis, erythema multiforme, and Sweet's syndrome (Sterling and Heymann, 2000). KI is usually administered in the form of a saturated solution at a dose of 0.3–6.0 g/day. As iodide concentrates in the salivary glands, the thyroid gland, the gastric mucosa, the mammary glands, the choroid plexus, and the placenta (Cavaliere, 1997), the use of KI with other potassium-containing drugs, potassium-sparing diuretics, and angiotensin-converting enzyme inhibitors can result in hyperkalemia and potassium toxicity (Medical Economics, 1998). In addition, the combination of KI with other iodide-containing drugs (e.g., amiodarone) and drugs that inhibit thyroid function (e.g., phenazone, lithium, and possibly sulfonamides) can cause hypothyroidism (Woerber, 1991). Indeed, patients taking KI frequently suffer from a number of side effects, including diarrhea, nausea, vomiting, and stomach pain

(Medical Economics, 1998). These effects can be eliminated by decreasing the dosage, however patients may also experience symptoms of potassium toxicity or iodism over long-term use.

In contrast, iodine is a microelement that plays a vital role in the development of brain activity and cell growth (Yaqoob et al., 2006). As an iodine deficiency can lead to miscarriages during pregnancy, deaf-mutism, and paralysis (Hassanien et al., 2003), additional iodine intake from iodine-rich foods or supplements is recommended. One of the most common dietary supplements is KI (Ratanawimarnwong et al., 2005), which is also the most common additive in iodized salt. However, excess iodine can also lead to different pathologies such as hyperthyroidism (Castillo et al., 2001), and so the detection and quantification of KI in different media, ranging from foodstuffs to biological liquids, is of great importance.

To date, a number of sensors both for potassium and iodine detection have been described in literature. However, to the best of our knowledge, only one sensor can simultaneously determine the K⁺ and I⁻ ion pair (Liu et al., 2010). This sensor is based on the use of fluorescent indicators that change their fluorescence intensity depending on the ion detected. However, as an ion concentration of 0.5 mM is required for this sensor, it is not suitable for use with biological

* Corresponding author at: Department of Chemistry, M.V. Lomonosov Moscow State University, 1–3 Leninskiye Gory, GSP-1, Moscow 119991, Russia.
E-mail address: puchninkv@yandex.ru (K. Puchnin).

samples, where the normal concentrations of I^- are $1.4\text{--}9.6 \times 10^{-7}$ M for human saliva (Bruger and Member, 1943) and $9.0\text{--}70.3 \times 10^{-6}$ M for human first morning urine (Rendl et al., 1994). There is therefore a necessity to develop a sensitive sensor for the determination of KI in biological samples.

Calixarene tubes (calixtubes), comprising two calixarene moieties linked by ethylene bridges, are effective and selective KI-binding ionophores (Schmitt et al., 1997). Indeed, iodide anions are considered to be the best counterions for complexation with calixarene tubes (Matthews et al., 2002). In addition, according to quantum chemistry calculations and X-ray crystallographic data, the binding of potassium cations occurs within a cryptand-like cavity in the ligand, where the guest cation travels via an axial path through one of the calixarene macrocycle rings (Felix et al., 2002).

Despite the advantages of employing calixarene tubes as active sensor components, no KI sensors based on this class of molecules have yet been developed. This may be due to the restricted modification options exhibited by calixarene tubes. However, to date, halogen-, alkyl- and aryl-substituted calixtubes (Schmitt et al., 1997; Matthews et al., 2002, 2003; Budka et al., 2002; Makha et al., 2002) have been synthesized. Although halogen-substituted calixtubes were synthesized to undergo subsequent transformation to amine or carboxyl substituents, subsequent development to yield halogenated derivatives has yet to be demonstrated. However, an alternative synthetic strategy towards calixarene tubes has been proposed recently, and involves the introduction of adamantyl derivatives to one or both calixarene rings (Puchnin et al., 2012). This method affords carboxyl, hydroxyl, and amine derivatives, among others, and so we selected adamantylated calixarene tubes for the purpose of this study.

The production of anchor group-containing derivatives for the covalent immobilization of calixarene tubes on oxide surfaces has also received significant interest for calixtube modification. For example, calixtube molecules carrying silatrane fragments are of particular interest. Silatranes are the products of the reaction between trialkoxysilane and triethanolamine, and their reactivities are significantly lower than those of the trialkoxysilane and trichlorosilane groups. This can be attributed to the positive mesomeric effect afforded by the shift of the lone electron pair from the nitrogen to the silicon atom (Frve et al., 1961). As a result, more uniform thin films can be generated and fewer conditions for reagent modification are required.

As the modification of calixarene tubes allows their efficient immobilization for practical applications, such as in the preparation of field effect transistor (FET)-based sensors, these sensors can be considered integrated devices containing a receptor layer that selectively recognizes and binds the target compound and a signal transducer, represented by an ion-selective field effect transistor (ISFET) that registers the recognition (Bergveld, 2003). The ISFET structure resembles that of a metal-oxide-semiconductor field effect transistor (MOSFET); however, an electrolyte solution is applied instead of a metal gate (Bergveld, 1970). Any process that takes place in the solution (pH or ionic strength alteration) or on the ISFET surface (specific adsorption) leads to a change in the surface potential and consequent modulation of the drain-source current in the transistor channel; this becomes the analytic signal of the sensor. In addition, ISFET sensors exhibit significant advantages over other signal transducers, including their small size, low manufacturing costs, low energy consumption, and the possibility of integration into signal processing systems for the construction of compact portable devices for express analysis. To date, ISFET-based sensors have been developed for the detection and analysis of various substances, including ions, small organic compounds, proteins, DNA, and living cell responses (Lee et al., 2009; Jimenez-Jorquera et al., 2010; Bronder et al., 2014). In our previous studies, we reported the development of ISFET-based biosensors for the detection of pesticides (Andrianova et al., 2016) and explosives (Komarova et al., 2015), thereby demonstrating their potential to detect interactions between calixarene tubes and target molecules.

Thus, we herein focus on the development of calixtube derivatives

comprising silatrane fragments, the formation of thin films based on these derivatives, subsequent modification of the FET surfaces with these derivatives, and finally, investigation into the sensory properties of the prepared ISFET.

2. Material and methods

2.1. Materials

All chemicals received from commercial sources were used without further purification. Solvents were purified and dried according to standard procedures. Calixtubes **1**, **2**, and **3** were synthesized according to published procedures (Puchnin et al., 2012).

Synthesis of APS: γ -Aminopropyltriethoxysilane (APTES, 4.42 g, 20 mmol) and triethanolamine (2.98 g, 20 mmol) were mixed in absolutized toluene (100 mL) and boiled in apparatus equipped with a Dean-Stark receiver over 3 h in the presence of metallic sodium (5 mg) as a catalyst. After this time, the solvent volume was reduced by half by evaporation and cooled in a refrigerator at 2 °C. The resulting precipitate was then filtered under a nitrogen atmosphere to afford the desired product as a white powder (3.54 g, 76% yield).

General Synthetic Procedure for calixtubes **4**, **5**, and **6** with silatrane anchor groups: The prepared calixtube (0.075 mmol) was dissolved in a 1:1 dry benzene: $SOCl_2$ mixture (4 mL) and gently heated to reflux ($T_{bath} \approx 90$ °C) with stirring over 2 h. After this time, the excess $SOCl_2$ was removed under reduced pressure and the residue was repeatedly re-evaporated with fresh benzene. The solid product was then dissolved in dry benzene (15 mL) and a solution of APS (0.45 mmol) in dry benzene (15 mL) was added dropwise with stirring. After removal of the solvent, CH_2Cl_2 (30 mL) was added and the solution was washed twice with H_2O (30 mL). The resulting solvent was filtered through filter paper and the residue reprecipitated from a CH_2Cl_2 -hexane solution to yield the desired calixtube products as white solids (Calixtube **4**: 93 mg, 45%; Calixtube **5**: 141 mg, 67%; Calixtube **6**: 78 mg, 53%).

2.2. NMR and mass spectral measurements

All NMR spectra were acquired at 25 °C on Bruker AVANCE 400 and AVANCE 600 spectrometers. Chemical shifts are reported in ppm referenced to solvent signals. In the ^{13}C NMR spectra, signal assignment was assisted by an attached proton test (APT) experiment. Calixtube **6**, comprising two silatrane fragments, was characterized as a potassium complex, which was obtained by the addition of excess solid KI to an NMR tube containing a $CDCl_3:CD_3OD$ (4:1) solution of the calixtube and by allowing the solution to stand until it equilibrated (1.5 w). High-resolution mass spectra (HRMS) were recorded on a Thermo Scientific LTQ Orbitrap instrument with electrospray ionization (see Supplementary material).

2.3. Monolayer preparation

The p-type silicon boron-doped wafer (Ameks, Russia) was cleaned with Caro solution followed by chemical etching in an HF-HCl solution. The cleaned surface was treated by plasma oxidation followed by annealing at 300 °C over 30 min. The prepared wafer was then cut into 8×8 mm slides. Prior to subsequent procedures, the slides were treated with UV-generated ozone in a BioForce UV/Ozone Pro-Cleaner ozone generator (USA) for 10 min to refresh the surface oxides.

The prepared slides were then submerged into a toluene solution of silatranated calixtubes (4 mg calixtube in 10 mL toluene) and incubated for 3 h at 70 °C, prior to rinsing with CH_2Cl_2 , and drying. An additional hydrolysis stage was introduced for fixation of the self-assembled monolayer (SAM) on the surface by heating the samples in a 0.6 vol% water-acetonitrile solution for 1 h at 70 °C with subsequent drying. The ISFET monolayers were prepared in a similar manner. The

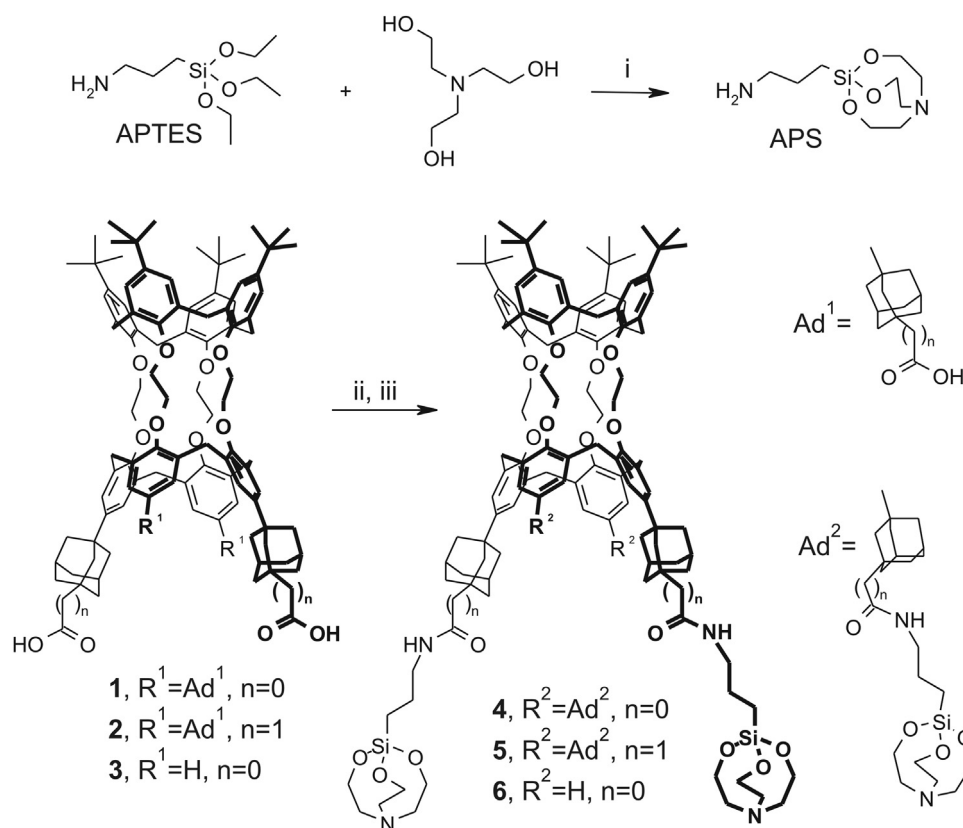


Fig. 1. Synthesis of calixtubes bearing silatrane anchor groups. (i) Na, toluene; (ii) SOCl_2 , benzene; (iii) aminopropyl silatrane (APS), benzene.

obtained films were then characterized by contact angle, atomic force microscopy (AFM), scanning electron microscopy-energy dispersive X-ray analysis (SEM-EDX), and X-ray photoelectron spectroscopy (XPS) measurements.

Water wetting contact angle measurements were conducted at room temperature (20 °C) using an OCA 15EC DataPhysics Instrument (Germany). Deionized water (electrical resistance = 18.2 M Ω cm) was dropped onto each surface, and the contact angles were assessed using SCA 20 software. Terminal values of the contact angles were taken as an average of three measurements on different parts of each sample.

The AFM study was performed on a Bruker Dimension ICON probe-scanning microscope (USA). Probes of the RTESPA series (Bruker, USA) in tapping mode were used to obtain the 3 × 3 μm (256 dots per line) images. Built-in functions of the Nanoscope Analysis software were used for image processing.

The elemental composition of the surface was studied using the energy dispersive X-ray analyzer at 10 kV (SEM JSM-6010LA (Japan)).

X-Ray photoelectron spectroscopy was employed to study chemical composition of deposited SAM (PHI VersaProbe II Scanning XPS Microprobe (USA)). XPS spectra were collected on calixtube **4** and **6**.

2.4. Chip formation

ISFET formation and packaging are described in detail in the literature (Gubanova et al., 2017). n-channel silicon-oxide silicon (SOI) ISFETs were manufactured at the SMC Technological Center, Russia according to the 1.2 μm CMOS process. Structures similar to FD (fully depleted) MOSFET but without poly-silicon gates and with a 100 × 100 μm channel were obtained in the silicon active layer thinned to 50–70 nm. The sensitive surface of the ISFET was a SiO_2 layer.

2.5. Sensor parameter measurements

The two structures formed on the ISFET were used during sensor

measurements, namely a well-like structure and a microfluidic system (MFS) (Fig. S12) (Gubanova et al., 2017). For the well-like structure, measurements were conducted with a working solution volume of 50 μL in the presence of a platinum reference electrode. Test solutions were added manually by pipetting 2 μL aliquots to reach the desired concentrations. For the MFS, flow regime measurements were conducted using an automatic dispensing system (neMESYS, Germany) at a constant flow rate of 1 $\mu\text{L s}^{-1}$ by continuous supply of the working solution with sequential switching to the test solution.

As a chemical sensor, ISFET was exploited in subthreshold mode. ISFET I–V characteristic curves (dependence of drain current (I_{DS}) on the reference electrode voltage (V_{GS})) were recorded using an Agilent B1500A semiconductor device parameter analyzer (USA) and a Cascade PM5 probe station (USA) with Agilent VEE Pro. Temporal changes in the subthreshold current I_{DS} at a constant appropriate V_{GS} and constant source-drain voltage ($V_{\text{DS}} = 0.1 \text{ V}$) were measured, and changes in the surface potential (i.e., the potential at the solution-oxide interface, $\Delta\phi_{\text{S}}$) at each point were calculated and used as the main parameters of the response to compound addition, as reported in the literature (Andrianova et al., 2016).

3. Results and discussion

3.1. Synthesis

Silatrane fragments were introduced into the calixarene tubes via the formation of an amide bond. This method was previously applied to the synthesis of organic dyes based on porphyrins, bipyridines, and other similar nitrogen-containing compounds (Brennan et al., 2013; Szpakowski et al., 2013; Mutneja et al., 2014). According to this method, amide bond formation is achieved through the initial synthesis of a carboxylic acid chloride followed by reaction with the corresponding amine. Thus, adamantylated calixarene tubes carrying carboxyl groups were selected as the starting materials, while γ -aminopropylsilatrane

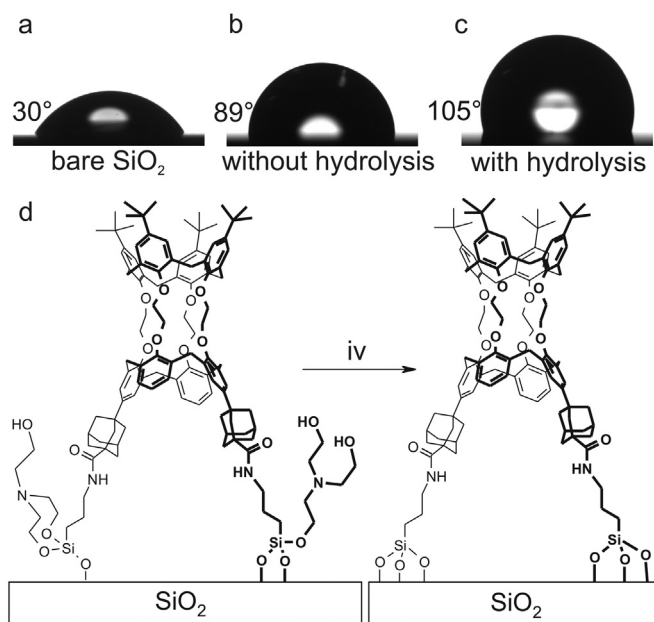


Fig. 2. Water-drop profiles on (a) the bare SiO₂ surface, (b) the calixtube **6**-modified SiO₂ surface without an additional hydrolysis stage, and (c) the calixtube **6**-modified SiO₂ surface with an additional hydrolysis stage. (d) The proposed structures of the molecules in the SAM both before and after the additional hydrolysis stage. (iv) H₂O, CH₃CN.

(APS) was selected as the amine due to its successful application in previous studies (Szpakowski et al., 2013; Mutneja et al., 2014; Li et al., 2000; Puri et al., 2011; Senapati et al., 2013; Guo et al., 2014).

Initially, calixtubes **1** and **2** (Fig. 1) comprising four carboxyl groups with varying spacer distances between them and the calixarene scaffold, were produced (Puchnin et al., 2012). These calixtube derivatives were selected for the simplicity of their preparation and characterization. Calixtube **3** (Fig. 1), comprising only two carboxyl groups, was also synthesized (Puchnin et al., 2012). This decrease in the number of carboxyl groups led to fewer silatrane fragments being introduced into the calixarene tubes, and so their frames will be less firmly fixed onto the surface compared to their tetracarboxylated analogs. This may result in different complexation parameters.

The conjugation reaction between the calixtubes and APS requires high purity starting materials, as any unreacted triethanolamine and APTES from the synthesis of APS in addition to any byproducts from their incomplete substitution (i.e., when one or two hydroxyl groups from triethanolamine did not react with APTES) can react with acyl chlorides via both their amino and hydroxyl groups. This dramatically increases the number of byproducts, complicating the purification process and decreasing the yield. Thus, to synthesize pure APS, we combined two techniques, namely reflux in toluene and the use of metallic sodium as a catalyst (Shlyakhtenko et al., 2003; Shi et al., 2005). The majority of toluene was then removed by evaporation following the reaction and the residue was cooled in a refrigerator at 2 °C. The resulting APS precipitate was filtered and stored under a nitrogen atmosphere to prevent hydrolysis of the product from atmospheric moisture.

The calixtube acid chlorides were prepared according to a common literature method without significant changes (Puchnin et al., 2012). The obtained acid chlorides were then reacted with APS in benzene without any additional purification. To remove any excess APS, the reaction mixture was extracted using a two-phase CH₂Cl₂-H₂O system, and the polymer byproducts were removed from the reaction mixture by filtration. The calixarene tubes were purified via reprecipitation from a CH₂Cl₂-hexane mixture. When reprecipitation was not sufficient, chromatographic purification was possible. However, this resulted in some loss of product due to interaction with the silica gel.

Using this method, calixarene tubes **4**, **5**, and **6** (Fig. 1) bearing silatrane fragments were successfully afforded.

All calixtubes were characterized by NMR spectroscopy and by HRMS. The time weighted symmetries of calixarene tubes **4** and **5** were characterized from a C_{2v} symmetry viewpoint due to the flattened cone-flattened cone slow conformational transition (Schmitt et al., 1997) that led to distinctive doublet NMR signals (Fig. S1-S4).

However, the NMR spectrum of calixtube **6** was more complicated owing to the nonequilibrium distribution between the flattened cone conformations that is inherent for almost all disubstituted calixarene tubes (Puchnin et al., 2013). NMR data revealed that calixtube **6** forms a complex with KI following prolonged incubation of a calixtube **6** solution in CDCl₃:CD₃OD (4:1) in the presence of excess KI. The spectrum of the resulting calixtube **6**·KI complex was much simpler than that of the corresponding free ligand due to fixation of the conformational transitions by the potassium cation located within the cryptand-like cavity of the molecule (Fig. S5-S7).

3.2. Formation and characterization of calixtube self-assembled monolayers (SAMs)

We then investigated the formation of calixarene tube-based SAMs on silicon slides bearing a surface silicon dioxide layer. The slide surface was initially treated with UV-generated ozone to remove any organic admixtures and to regenerate free hydroxyl groups on the surface to provide maximum dense immobilization of the calixtube molecules. Since calixarene tubes must be oriented with the *tert*-butyl groups facing “up” (i.e., off the surface), the surface should become hydrophobic after successful formation of the desired SAM. Thus, a preliminary estimation of SAM formation was performed by measuring the water wetting contact angle. Thus, the calixarene tubes were attached to the surface by prolonged heating of the slides in a calixtube-toluene solution, and optimization of the conditions demonstrated that dispersion of the resulting contact angle value significantly decreased for an incubation period ≥3 h at 70 °C, likely due to termination of the SAM film formation process. However, an increase in temperature complicated the reaction process due to significant solvent evaporation, while a decrease in temperature decelerated SAM formation. Calixtube **4** films formed under these conditions exhibited a contact angle of 92 ± 2° compared to 30 ± 3° for the bare SiO₂ surface (Fig. 2a). Similarly, calixtubes **5** and **6** displayed contact angles of 91 ± 2° and 89 ± 2°, respectively (Fig. 2b).

Hydrolysis of the silatrane fragment following binding of the calixtubes (with the silatrane anchor groups) to the surface was then carried out. The first stage (i.e., Si-OCH₂ hydrolysis) was relatively fast; this was followed by a slower stage comprising hydrolysis of the second and third Si-OCH₂ bonds (Shlyakhtenko et al., 2013). This difference in reactivities led to the formation of imperfect films, where the surface exhibited the target molecules in addition to attached triethanolamine residues displaying free OH-groups. Thus, a decrease in the contact angle was observed compared to the perfect films (Fig. 2d). To remove the triethanolamine residues and achieve enhanced fixation of the target molecules on the surface, we introduced an additional hydrolysis stage by heating the samples in a 0.6 vol% water-acetonitrile solution (Brennan et al., 2013). This resulted in an increased contact angle of 105 ± 3° (Fig. 2c).

The morphology of the resulting films was then investigated by AFM (Fig. S8). Following incubation of the SiO₂ surface for 3 h in a solution of calixtube **4**, a smooth film with a roughness R_a = 0.154 ± 0.033 nm was obtained, where the R_a of the initial SiO₂ surface was determined to be ~0.12 nm. Calixtubes **5** and **6** also produced uniform smooth films.

Energy dispersive X-ray analysis showed the presence of C (about 9 atom %) on the background of a large signal of Si (about 90 atom %). Such a large signal of the substrate in comparison with the signal of a thin film is due to the small thickness of SAM (Fig. S9).

XPS analysis also confirmed the immobilization of calixtubes on the surface. It turned out that part of the silatrane groups underwent hydrolysis incomplete (left part of the Fig. 2d), as evidenced by the presence of the peak of the N1s (1) C–N bond corresponding to triethanolamine (Fig. S10, S11 and Table S1, S2).

These data therefore confirm that the calixarene tubes form a hydrophobic film on the surface of oxidized silicon chips, where the wetting contact angle of the film is determined by the terminal *tert*-butyl groups present in the calixarene tube moieties.

3.3. FET modification

The developed method for immobilization of the calixarene tubes on the SiO₂ surface was then applied to construction of the ISFET-based sensor. The FET-sensitive surface was modified in the same way as the SiO₂ surface to produce three different ISFET modifications, each with a different layer of calixtubes. To operate sufficiently with solutions during testing of the unpackaged modified ISFETs, a well-like structure was formed on the surface during the preliminary study. Packaged chips with integrated microfluidics were then created for terminal evaluation of the sensoric properties (Fig. S12).

3.4. Sensoric properties of the modified FET

A 1×10^{-2} M ammonium acetate solution (pH 7), often used as the working solution in experiments with ISFET sensors for Ca²⁺ (Mlika et al., 1997), Na⁺, and Ni²⁺ (Mlika et al., 1998), was applied as the working solution in our experiments.

To test the response of the ISFET to KI addition, the signals from the modified and non-modified transistors were compared. Aliquots of KI with final concentrations of 3.8×10^{-5} and 4.2×10^{-4} M were added to the original and calixtube 4-modified ISFETs, and the response times were estimated from the output of the signal to the plateau (i.e., ≤ 200 s). The obtained registration curves indicated that the addition of KI to a modified transistor leads to an increase in its surface potential $\Delta\phi_s$, while the same addition to a non-modified transistor produces no response. This increase occurs because the immobilized calixarene tubes form a complex with KI, consequently increasing the local concentration of ions close to the surface, thereby leading to a direct change in the surface potential. This experiment demonstrated the potential of calixtube-modified ISFETs for use as KI sensitive sensors.

The selectivity of the afforded sensor to cations was then examined via the application of different alkali metal iodide solutions, namely NaI, KI, RbI, and CsI. The response of the ISFET to KI exhibited the largest value (30 mV at 3.8×10^{-5} M KI and ~ 50 mV at 4.2×10^{-4} M), which was attributed to the ability of the calixarene tube to form a complex with the ions via its cryptand-like cavity (formed by the phenyl oxygen atoms). The addition of other iodides also afforded a response from the sensor (Fig. 3); however, this response was significantly weaker and was approximately equal in all cases (surface potential increase = ~ 7 mV at 3.8×10^{-5} M iodide concentration and ~ 20 mV at 4.2×10^{-4} M). This can be associated with the formation of complexes between the aromatic cavity of the calixarene ring and large cations, such as Rb⁺ or Cs⁺. Although the smaller Na⁺ ions form potassium similar complexes via the cryptand-like cavity of the calixtubes. These complexes are significantly weaker strong due to the absence of the template effect caused by size disparity. This leads to a smaller change in the local concentration close to the transistor surface for NaI, RbI, and CsI when compared to that of KI, and so a lower sensor response is observed for these metal iodides.

As the binding of a potassium cation with calixarene tubes in a chloroform-methanol medium strictly depends on the counterion employed (Matthews et al., 2002), we examined the influence of the counterion on the calixtube-modified transistor with the addition of 3.8×10^{-5} M potassium acetate, iodide, nitrate, chloride, dihydrophosphate, and perchlorate solutions in a 1×10^{-2} M ammonium acetate

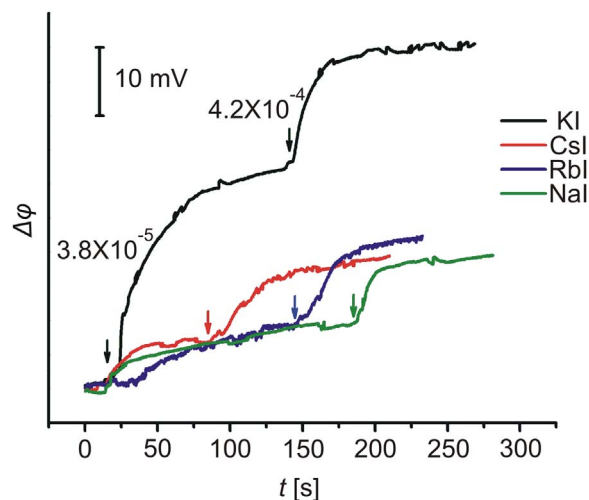


Fig. 3. Response of the calixtube 4-modified ISFET to the addition of different alkali metal iodide solutions: 3.8×10^{-5} M solutions added at 20 s and 4.2×10^{-4} M solutions added at the times indicated by the colored arrows. A 1×10^{-2} M ammonium acetate working solution was also employed.

working solution. Potassium iodide afforded the highest response (100%) (Table 1), followed by potassium acetate (26.6%), potassium perchlorate (15.6%), potassium dihydrophosphate (8.9%), and potassium nitrate (3.1%). The response of the calixarene tube-modified ISFET sensor to KCl was negligible.

The effect of KI concentration on the surface potential ($\Delta\phi_s$ -[KI]) of calixtubes 4, 5, and 6 was then investigated, and all sensors exhibited comparable limits of detection for KI ($\sim 5 \times 10^{-6}$ M) regardless of the type of calixarene tube immobilized on the surface. This demonstrates that a slight alteration in the bridge spacer length (i.e., between calixtubes 4 and 5) or the number of silatrane anchor groups (i.e., between calixtubes 4 and 6) has a negligible influence on the sensoric parameters of the modified ISFET. These results therefore suggested that the exhibited ionophore properties of the produced SAM are caused by the terminal *tert*-butyl groups on the upper rims of the calixarene tubes in addition to the size of the distal calixarene macrocycle. Thus, the ionophore properties of the immobilized calixtubes can be varied by changing the size of the macrocycle (for example, by coupling different calixarenes to an asymmetric calixtube comprising a thiacalixarene fragment) (Khomich et al., 2006) or by replacing the terminal *tert*-butyl group.

To estimate the suitability of applying this sensor for KI analysis in real samples, the analysis of artificial KI-containing saliva was examined. As shown in Fig. 4a, the addition of KI-containing saliva to KI-free saliva afforded a distinctive response from the modified transistor. The limit of detection for the sensor under such conditions was determined to be $\sim 3 \times 10^{-8}$ M (Fig. 4b).

3.5. Combination of the modified ISFET with a microfluidic system (MFS)

To achieve accurate and facile analyte delivery, the ISFET was combined with a microfluidic system (MFS), which results in lower analyte volumes and automated sample preparation, thereby minimizing the requirement for human intervention during analysis.

Table 1
Response of the calixtube 4-modified ISFET sensor to different potassium salt solutions (3.8×10^{-5} M) in comparison to its response to potassium iodide. A 1×10^{-2} M ammonium acetate working solution was also employed.

KI	CH ₃ COOK	KClO ₄	KH ₂ PO ₄	KNO ₃	KCl
1	0.266	0.156	0.089	0.031	0.008

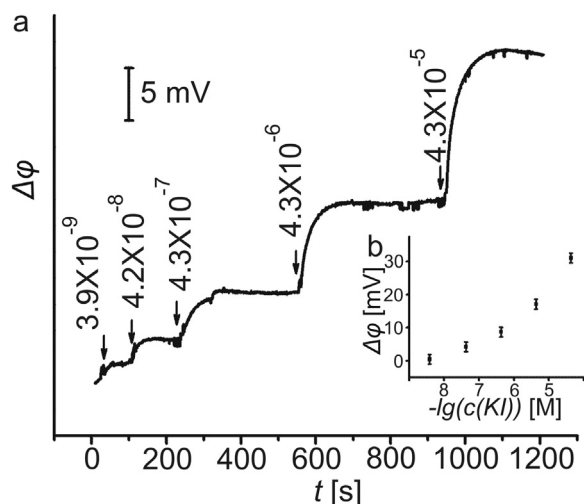


Fig. 4. (a) Response of the calixtubane 6-modified ISFET to the addition of KI solutions with concentrations ranging from 3.9×10^{-9} to 4.3×10^{-5} M (final). Artificial saliva = urea 2 mM, glucose 0.02 g/L, KCl 20 mM, BSA 4 g/L, NaCl 10 mM, CaCl_2 2 mM, MgCl_2 0.6 mM, NH_4Cl 1.8 mM. (b) The semi-logarithmic dependence of the calixtubane 6-modified ISFET response to the KI concentration (relative error < 10%).

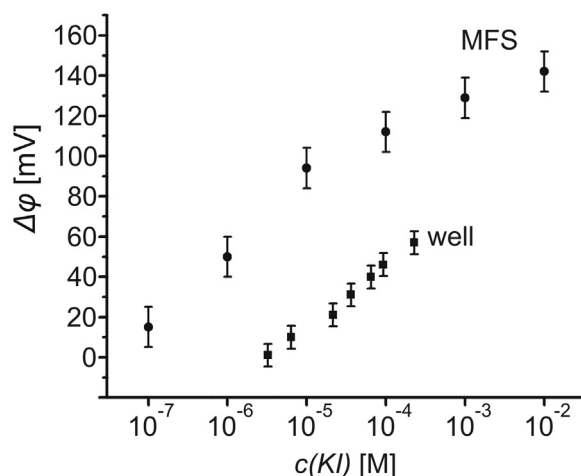


Fig. 5. Semi-logarithmic dependence of the calixtubane 5-modified ISFET response to KI concentration for the well-like (squares) and microfluidic system (MFS)-like (circles) measurement structures (relative error < 10%). A 1×10^{-2} M ammonium acetate working solution was also employed.

The MFS was fabricated on top of the packaged ISFET (Gubanova et al., 2017), and the ISFET surface was modified with calixtubane 5. Measurements were performed in flow mode with an automatic dispensing system as follows: the sensor was exposed to a constant flow rate of the 1×10^{-2} M ammonium acetate working solution with subsequent addition of KI to the desired concentration (i.e., 10^{-9} to 10^{-2} M). After each measurement, the MFS was rinsed with the working solution. The KI limit of detection for the MFS system was 10^{-7} M, which is higher than that observed for the well-like system, thereby providing a wider linear response range of 10^{-7} to 10^{-2} M (Fig. 5). A decrease in the volume of the reaction mixture may therefore influence the LoD of the sensor in the case of a 50 μL well-like system and a 1 μL chamber in the MFS placed just above the ISFET surface.

The LoD of the developed sensor towards KI therefore appears comparable to the LoDs of other sensors towards iodine (i.e., 1.1×10^{-7} M (Ohashi et al., 2000), 1.42×10^{-7} M (Dunn et al., 2009), and 2×10^{-7} M (Knowles and Lowden, 1953)). It was therefore apparent that we had successfully constructed a sensor based on calixtubanes and an n-channel ISFET for the detection of KI. We expect that the LoD of this biosensor could be reduced by replacement of the SiO_2 layer with

Ta_2O_5 (Eickhoff et al., 2003). In addition, the sensor presented herein is CMOS-compatible, which renders it inexpensive and enables combination with other signal processing devices and interfacing microelectronic technologies.

4. Conclusions

A series of calixarene tubes with silatrane anchor groups was synthesized in satisfactory yields using the amide bond method. Thus, a self-assembled monolayer (SAM) based on calixtubanes was produced for the first time using a SiO_2 surface, and the preparation conditions were determined (i.e., 3 h incubation of the surface in a silatrane-doped calixtubane solution in toluene at 70°C). An additional hydrolysis stage (i.e., heating of the samples in a 0.6 vol% water-acetonitrile solution) was also necessary to achieve fixation of the developed SAM on the SiO_2 surface.

Modification of the ISFET sensitive surface with calixtubanes enabled the fabrication of a sensor sensitive to the KI ion pair. This sensor selectively determined KI compare to different alkali metal iodides: NaI, RbI, CsI; also investigation of different potassium salts (acetate, iodide, nitrate, chloride, dihydrophosphate, perchlorate) showed the highest response to KI. The limits of detection of the resulting sensor towards KI were determined to be 5×10^{-6} M for the well-like measurement structure and 1×10^{-7} M for the microfluidic system in 1×10^{-2} M ammonium acetate. Due to selectivity and potential for the determination of KI in artificial saliva (the LoD is $\sim 3 \times 10^{-8}$ M), the constructed sensor exhibits great potential for application in the determination of KI in different media, such as the human body, and certain biological samples, including saliva and urine.

Acknowledgements

This project was supported by the Russian Ministry of Education (project no 16.9183.2017_B4). We thank the Center of Collective Use “Functional Control and Diagnostics of Micro- and Nanosystem Engineering based on R&D Technological Center” (Moscow) for allowing access to their equipment.

Appendix A. Supporting information

Supplementary data associated with this article can be found in the online version at doi:10.1016/j.bios.2017.06.050.

References

- Andrianova, M.S., Gubanova, O.V., Komarova, N.V., Kuznetsov, E.V., Kuznetsov, A.E., 2016. *Electroanalysis* 28, 1311–1321.
- Bergveld, P., 1970. *IEEE Trans. Biomed. Eng.* 17, 70–71.
- Bergveld, P., 2003. *Sens. Actuators B* 88, 1–20.
- Brennan, B.J., Llansola Portolés, M.J., Liddell, P.A., Moore, T.A., Moore, A.L., Gust, D., 2013. *Phys. Chem. Chem. Phys.* 15, 16605–16614.
- Bronder, T., Wu, C.S., Poghosian, A., Werner, C.F., Keusgen, M., Schöning, M.J., 2014. *Procedia Eng.* 87, 755–758.
- Bruger, M., Member, S., 1943. *Am. J. Physiol.* 139, 212–216.
- Budka, J., Lhoták, P., Štibor, I., Michlová, V., Šykora, J., Cisarová, I., 2002. *Tetrahedron Lett.* 43, 2857–2861.
- Castillo, V.A., Pisarev, M.A., Lalia, J.C., Rodriguez, M.S., Cabrini, R.L., Márquez, A.G., 2001. *Vet. Q.* 23, 218–223.
- Cavalieri, R.R., 1997. *Thyroid* 7, 177–181.
- Dunn, J.T., Crutchfield, H.E., Gutekunst, R., Dunn, A.D., 2009. *Thyroid* 3, 119–123.
- Eickhoff, M., Schalwig, J., Steinhoff, G., Weidemann, O., Görgens, L., Neuberger, R., Hermann, M., Baur, B., Müller, G., Ambacher, O., Stutzmann, M., 2003. *Phys. Status Solidi C Conf.*, 1908–1918.
- Felix, V., Matthews, S.E., Beer, P.D., Drew, M.G., 2002. *Phys. Chem. Chem. Phys.* 4, 3849–3858.
- Frve, C.L., Vogel, G.E., Hall, J.A., 1961. *J. Am. Chem. Soc.* 83, 996–997.
- Gubanova, O., Andrianova, M., Saveliev, M., Komarova, N., Kuznetsov, E., Kuznetsov, A., 2017. *Mater. Sci. Semicond. Process.* 60, 71–78.
- Guo, P., Wang, Y.-W., Luo, X.-T., Qi, X.-L., Hou, L.-P., Xie, Z.-X., Ye, F.-Q., 2014. *Phosphorus Sulfur Silicon Relat. Elem.* 189, 511–518.
- Hassani, M.H., Hussein, L.A., Robinson, E.N., Preston Mercer, L., 2003. *J. Nutr. Biochem.* 14, 280–287.

- Jimenez-Jorquera, C., Orozco, J., Baldi, A., 2010. *Sensors* 10, 61–83.
- Khomich, E., Kashapov, M., Vatsouro, I., Shokova, E., Kovalev, V., 2006. *Org. Biomol. Chem.* 4, 1555–1560.
- Knowles, G., Lowden, G.F., 1953. *Analyst* 78, 159–164.
- Komarova, N.V., Andrianova, M.S., Gubanova, O.V., Kuznetsov, E.V., Kuznetsov, A.E., 2015. *Sens. Actuators B* 221, 1017–1026.
- Lee, C.-S., Kim, S.K., Kim, M., 2009. *Sensors* 9, 7111–7131.
- Li, Z., Tian, D., Zhu, C., 2000. *Phosphorus Sulfur Silicon Relat. Elem.* 165, 99–105.
- Liu, Y.-L., Palacios, M.A., Anzenbacher, P., 2010. *Chem. Commun.* 46, 1860–1862.
- Makha, M., Nichols, P.J., Hardie, M.J., Raston, C.L., 2002. *J. Chem. Soc. Perkin Trans. 1*, 354–359.
- Matthews, S.E., Felix, V., Drew, M.G., Beer, P.D., 2003. *Org. Biomol. Chem.* 1, 1232–1239.
- Matthews, S.E., Schmitt, P., Felix, V., Drew, M.G., Beer, P.D., 2002. *J. Am. Chem. Soc.* 124, 1341–1353.
- Medical Economics Co, 1998. *Physicians desk reference*. 52nd ed. Montvale, p. 2947.
- Mlika, R., Ben Ouada, H., Hamza, M.A., Gamoudi, M., Guillaud, G., Jaffrezic-Renault, N., 1997. *Synth. Met.* 90, 173–179.
- Mlika, R., Ouada, H.B., Jaffrezic-Renault, N., Dumazet, I., Lamartine, R., Gamoudi, M., Guillaud, G., 1998. *Sens. Actuat. B* 47, 43–47.
- Mutneja, R., Singh, R., Kaur, V., Wagler, J., Kroke, E., 2014. *Dyes Pigm.* 108, 41–49.
- Ohashi, T., Yamaki, M., Pandav, C.S., Karmarkar, M.G., Irie, M., 2000. *Clin. Chem.* 46, 529–536.
- Puchnin, K., Cheshkov, D., Zaikin, P., Vatsouro, I., Kovalev, V., 2013. *New J. Chem.* 37, 416–424.
- Puchnin, K., Zaikin, P., Cheshkov, D., Vatsouro, I., Kovalev, V., 2012. *Chem. Eur. J.* 18, 10954–10968.
- Puri, J.K., Singh, R., Chahal, V.K., 2011. *Chem. Soc. Rev.* 40, 1791–1840.
- Ratanawimarnwong, N., Amornthammarong, N., Choengchan, N., Chaisuwan, P., Amatongchai, M., Wilairat, P., McKelvie, I.D., Nacapricha, D., 2005. *Talanta* 65, 756–761.
- Rendl, J., Seybold, S., Börner, W., 1994. *Clin. Chem.* 40, 908–913.
- Schmitt, P., Beer, P.D., Drew, M.G., Sheen, P.D., 1997. *Angew. Chem., Int. Ed. Engl.* 36, 1840–1842.
- Senapati, S., Manna, S., Lindsay, S., Zhang, P., 2013. *Langmuir* 29, 14622–14630.
- Shi, D.Q., Chen, Q., Li, Z.H., Liu, X.P., 2005. *Phosphorus Sulfur Silicon Relat. Elem.* 180, 1621–1627.
- Shlyakhtenko, L.S., Gall, A.A., Filonov, A., Cerovac, Z., Lushnikov, A., Lyubchenko, Y.L., 2003. *Ultramicroscopy* 97, 279–287.
- Shlyakhtenko, L.S., Gall, A.A., Lyubchenko, Y.L., 2013. *Cell Imaging Techniques. Methods and Protocols*. In: Taatjes, D.J., Roth, J. (eds.) Humana Press, New York, pp 295–312.
- Sterling, J.B., Heymann, W.R., 2000. *J. Am. Acad. Dermatol.* 43, 691–697.
- Szpakolski, K., Latham, K., Rix, C., Rani, R.A., Kalantar-zadeh, K., 2013. *Polyhedron* 52, 719–732.
- Woeber, K.A., 1991. *Med. Clin. N. Am.* 75, 169–178.
- Yaqoob, M., Atiq-ur-Rehman, Waseem, A., Nabi, A., 2006. *Luminescence* 21, 221–225.